THE JOURNAL OF PHYSICAL CHEMISTRY Letters

pubs.acs.org/JPCL

Crowding Effects on Amyloid Aggregation Kinetics

Andrea Magno, Amedeo Caflisch,* and Riccardo Pellarin*

Department of Biochemistry, University of Zürich, Winterthurerstrasse 190, CH-8057 Zürich, Switzerland

ABSTRACT Biological protein self-assembly occurs in the cellular milieu, densely occupied by other macromolecules which do not participate directly in the aggregation process. Excluded volume effects arising in such a crowded environment deeply affect the thermodynamics and kinetics of biological processes, like protein folding, ligand binding, and protein aggregation. Here, Langevin dynamics simulations of a simplified model of an amphipathic polypeptide are used to investigate how macromolecular crowding influences the amyloid aggregation kinetics. The simulations show that the net influence of macromolecular crowding on the self-assembly process is the result of two competing effects: oligomer stabilization and solution viscosity increase. Notably, the net effect crucially depends on the aggregation propensity and pathways. Therefore, comparative studies of concentration and crowding effects on the kinetics of amyloid aggregation could shed light on the underlying self-assembly mechanism.

SECTION Biophysical Chemistry

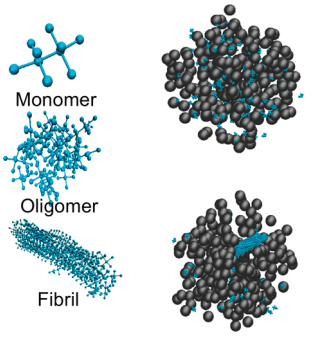

Amyloid fibrils are ordered polypeptide aggregates that have been related to several neurodegenerative pathologies, such as Alzheimer's, Parkinson's, Huntington's and prion diseases,[1,2] and, more recently, also to biological functionalities.[3,4] These findings have paved the way to a wide range of experimental and computational studies aimed at understanding the details of the fibril formation mechanism.

Most of these investigations were usually performed in ideal homogeneous conditions, though the actual cellular milieu is a much more complex environment. Several studies have pointed out the effects of geometric confinement on fibril formation and protein folding.[5,6] A universal property of the cells is that they are crowded.[7,8] Indeed, it has been estimated that 20−30% of the cell cytoplasm is occupied by proteins, RNA, membranes, polysaccharides, and several organelles.[9] Although the concentration of every species is low, these macromolecules exclude a significant fraction of the total available volume.[10] The nonspecific excluded volume effect is expected to sensibly affect all biological reactions in which proteins are involved.[11] Using scaled particle theory,[12] Minton and Ellis have predicted that macromolecular crowding dramatically increases the association rate of proteins and the relative stability of the unfolded and native state.[13,14] Computational studies have shown that the presence of inert, repulsive cosolutes stabilizes the native, compact state of proteins[15,16] and that the presence of nanoparticles is able to catalyze amyloid aggregation.[17] Experiments[18−21] conducted with large and weakly interacting macromolecules such as polyethyleneglycol (PEG) and Fycoll have confirmed these theoretical predictions, showing that the excluded volume effect is able to modify the subtle equilibrium between the folded, functional state and aberrant structures prone to aggregation.

Earlier, a very simple coarse-grained model of an aggregation-prone, amphipathic peptide was developed to investigate the kinetics of ordered aggregation.[22] The peptide monomer has a single degree of freedom, and the relative free-energy profile has only two minima, corresponding to the aggregation-prone and aggregation-protected states. By varying a single parameter of the model, that is, by reducing the β-aggregation propensity, the roughness of the free-energy landscape and the heterogeneity of the fibril elongation pathway increase. In previous simulation studies, heterogeneous kinetics of aggregation and multiple pathways were observed in bulk solution and in the presence of lipid bilayers. At high amyloidogenic conditions, the process of fibril formation is downhill and fast, whereas at low amyloidogenic conditions, several intermediates are detected, and the nucleation occurs through a micellar oligomer.[23] It has also been pointed out that amyloidogenicity determines the effect on peptide aggregation of the presence of lipid bilayer; while aggregation-prone peptides fibrillate faster by adsorbing on the bilayer surface, the ordered self-assembly of poorly amyloidogenic peptides is hindered by the vesicles.[24,25] In this work, a spherical model of softly repulsive crowders is used, together with the simple model of the amphipathic peptide, to investigate amyloid aggregation kinetics at different concentrations of crowders. It is found that the influence of the crowders has a pronounced dependence on the amyloidogenic tendency of the peptide.

The simulations were performed with 125 peptides and a number of softly repulsive crowders ranging from 250 to 5000 (see Methods and Table 1). Snapshots of the simulation

Received Date: July 16, 2010
Accepted Date: September 12, 2010

DOI: 10.1021/jz100967z | *J. Phys. Chem. Lett.* **2010**, *1*, 3027–3032

Table 1. Excluded Volume Fraction (ϕ), Equivalent Concentration (C_{eq} = 8.5 mM /(1 − ϕ)), and Peptide Self-Diffusion Coefficient ($\mathcal{D}$) at Different Crowder Contents n_C[a]

n_C	ϕ	C_{eq} (mM)	$\mathcal{D}$ (Å^2/ps)
250	0.066	9.10	1835
500	0.13	9.77	1765
1000	0.25	11.3	1435
1500	0.36	13.3	1234
2000	0.46	15.8	1075
2500	0.56	19.1	910
3000	0.64	23.4	779
3500	0.71	29.2	686
4000	0.77	37.1	617
4500	0.82	48.2	547
5000	0.87	64.2	498

[a]See the Methods section for details.

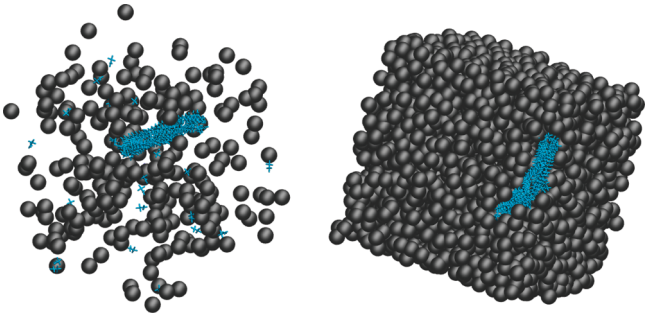

Figure 1. Snapshots of simulation systems at low (n_C = 250, left) and high crowder concentrations (n_C = 3000, right). Peptides are shown in a stick model in cyan, while crowders are black spheres.

system with a low (n_C = 250) and high (n_C = 3000) number of crowders are shown in Figure 1.

To compare crowding effects with an increase in peptides concentration, simulations in the absence of crowders with 125 peptides and a progressively decreasing volume of the simulation box (yielding peptide concentrations ranging from 8.5 to 61.5 mM) were also carried out. For each of these conditions, multiple runs were started (with different initial velocities) for each of four values of the amyloidogenicity (i.e., dE = −2.5, − 2.25, − 2.0, and −1.5 kcal/mol; see Methods for details) to investigate the dependence on the aggregation propensity. The temperature in all simulations was 310 K.

Crowders Effect on Lag Phase. Supercritical oligomers are assemblies whose size is larger than the nucleus, where the nucleus is defined as the oligomer that has a 50% probability to form a fibril[22] (see Methods and Table S1 (Supporting Information) for details). To specifically assess how macromolecular crowding influences the nucleation kinetics, the number of supercritical oligomers has been calculated as a function of time along each simulation (Figure 2). During the lag phase, the number of oligomers of supercritical size is roughly zero, that is, only small oligomers or monomers are present in the system, while for long time, only one aggregate, which corresponds to the mature fibril, is present. At intermediate times, the number of oligomers of supercritical size

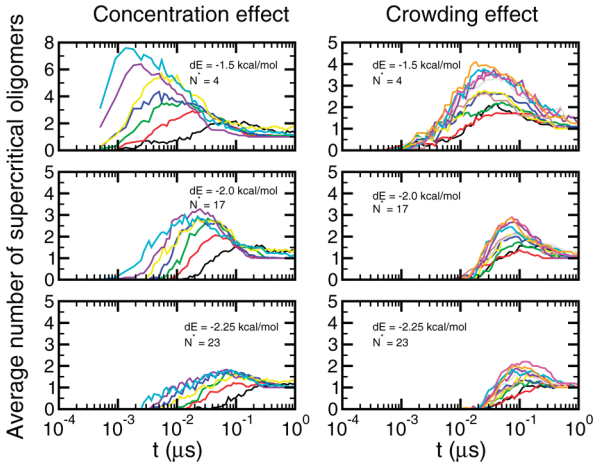

Figure 2. Peptide concentration but not crowder content accelerates the nucleation step. Average number of supercritical oligomers (i.e., with size larger than the nucleus aggregation number N^*) as a function of simulation time. Each curve is an average over 10 runs. The size N^* of the nucleus increases upon destabilization of the amyloid prone state (see Table S1, Supporting Information). (Left panels) Different colors represent different peptide concentrations, ranging from (black) C = 8.5 to (cyan) 61.5 mM. Note that the y-axis range is different for the top plot. (Right panels) Different colors represent different crowder contents, ranging from (black) n_C = 250, C_{eq} = 9.1 to (orange) n_C = 5000, C_{eq} = 64.2.

can be higher than one when two or more elongating fibrils are present simultaneously in the simulation box. To directly compare the effect of peptide concentration and macromolecular crowding, the equivalent concentration C_{eq}, defined as the ratio between the number of peptides and the volume unoccupied by crowders (see Methods), is introduced. Concentration increment and macromolecular crowding have sensibly different effects. They both increase the average number of supercritical oligomers at intermediate times, but the concentration also accelerates the nucleation step (corresponding to the shift of the peak toward shorter times in the time series in Figure 2, left), while the crowding has a much less pronounced influence on the nucleation step because the decrease in peptide diffusivity limits monomer encounters.

The mean first appearance of a supercritical oligomer t_{N^*} reports on the length of the lag phase. Crowding and concentration effects yield similar lag phases only for the peptide model with the lowest amyloidogenicity (Figure 3, left). On the contrary, for the more amyloidogenic peptide models, the lag phase becomes shorter by raising the concentration while it is only marginally influenced by the crowder content (Figure 3, right).

Crowders Effect on Oligomers Stability. To interpret the kinetics at low dE, it is useful to investigate the stability of oligomers that are competent to fibril nucleation and are explored during the lag phase. The presence of a large amount of inert macromolecules that exclude volume to peptides favors association.[14] Since oligomers are more compact than an equivalent amount of dispersed monomers, they are thermodynamically stabilized by an increase of excluded volume. Therefore, to study the thermodynamic properties of the metastable oligomers that appear during the lag phase, multiple simulations were carried out at different crowder

DOI: 10.1021/jz100967z | J. Phys. Chem. Lett. 2010, 1, 3027–3032

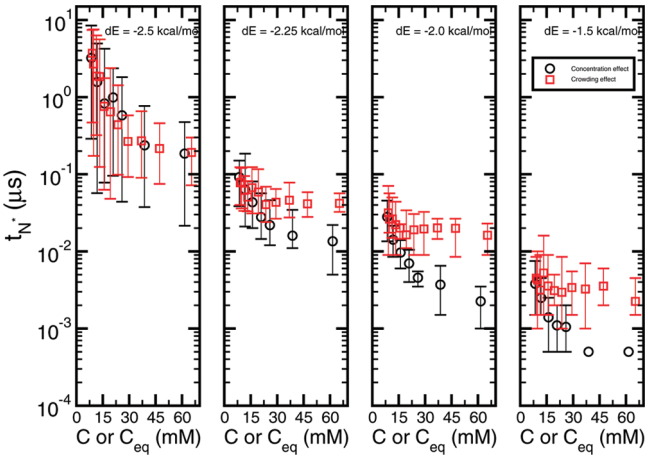

Figure 3. Time of appearance of the first supercritical oligomer t_{N^*}. Black circles are t_{N^*} values calculated at different peptide concentrations without crowders, whereas red squares are t_{N^*} values at different equivalent concentrations C_{eq} obtained by varying the number of crowders (see Table 1). Symbols represent the average value of 10 independent runs, and the error bars are the minimum and maximum values. Note that the two data points at highest peptide concentration (black circles) in the right panel do not have an error bar as the first supercritical oligomer appeared within the first coordinate saving interval of 0.5 ns.

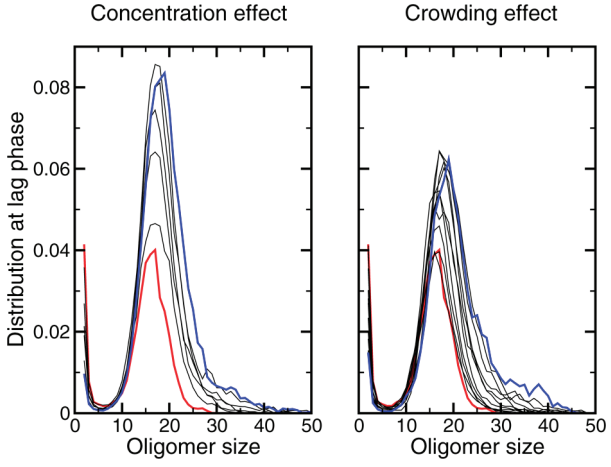

Figure 4. The increase in oligomer size is more pronounced for higher peptide concentration than that for higher crowding content. Oligomer size distribution, evaluated for $dE = -3.5$ kcal/mol, at different values of the crowder content and peptide concentration. The red curve in each plot corresponds to $C = 8.5$ mM ($n_C = 0$), while the blue curves correspond to the highest values of concentration ($C = 61.5$ mM and $C_{eq} = 64.2$ mM in the left and right panel, respectively). The frequency of the isolated monomers ranges from 0.64 to 0.12 and 0.64 to 0.31 on the left and right plots, respectively, and is not shown to avoid compression of the oligomeric peak.

concentrations with 125 peptides with a stable aggregation-protected state ($dE = -3.5$ kcal/mol). This value has been chosen to inhibit the fibril nucleation but not the oligomer formation. The distribution of oligomer sizes at different crowder concentrations shows that larger oligomers are stabilized by the excluded volume effect, which is proportional to the amount of crowders (see Figure 4). Therefore, macromolecular crowding stabilizes oligomers, but it does so

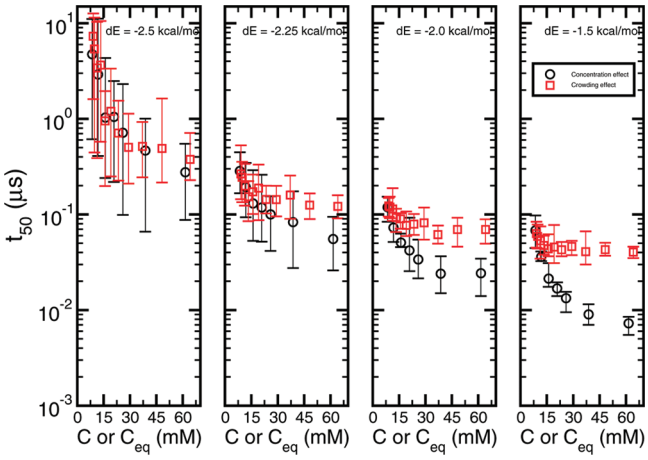

Figure 5. Differences in aggregation kinetics upon raising the peptide concentration or crowder content depend on amyloidogenicity. The time t_{50} at which the growing fibril has reached 50% of the polar contacts of the mature fibril is shown as a function of concentration. Black circles are t_{50} values calculated at different peptide concentrations in the absence of crowders, while red squares are t_{50} values at different equivalent concentrations C_{eq} obtained by varying the number of crowders (see Table 1). Symbols represent the average value of 10 independent runs, and the error bars are the minimum and maximum values.

less than an equivalent increase of peptide concentration. It has been shown experimentally that oligomeric intermediates can be stabilized significantly by macromolecular crowding.[19] In this context, it is likely that if off-pathway oligomers are present in the aggregation mechanism, the aggregation kinetics will be slowed down by crowding. Such an effect is not observed because off-pathway oligomers cannot be reproduced by the simple model used in this simulation study.

Crowders Effect on Fibril Formation Kinetics. Macromolecular crowding is more effective for the less aggregating peptides ($dE = -2.5$ kcal/mol), for which the time needed to establish half of the number of polar contacts present in the mature fibril (t_{50}) diminishes by an order of magnitude at high excluded volume fractions (Figure 5). This trend is analogous to that observed experimentally by Munishkina et al., who have studied the effect of increasing the PEG concentration on the α-synuclein aggregation process.[18] Note that the time t_{N^*} (shown in Figure 3) reports on the lag phase, while t_{50} is a mixed measure of both the lag phase and the inverse rate of elongation. Specifically, the t_{50} is dominated by the lag phase for low amyloidogenic peptide models because the nucleus size contains almost as many monomers as half of the final fibril. In contrast, it mainly reflects the inverse rate of elongation for high amyloidogenicity potentials whose nucleus size is very small.

The effect of macromolecular crowding is less pronounced for the more aggregating peptides, for which the t_{50} values reach a plateau already at low crowder content. Interestingly, for the peptide models with low aggregation propensity ($dE = -2.5, -2.25$ kcal/mol), the effect of macromolecular crowding and peptide concentration is similar (Figure 5, left). In contrast, for peptides more prone to aggregation ($dE = -2.0, -1.5$ kcal/mol), the acceleration of self-assembly promoted

DOI: 10.1021/jz100967z | J. Phys. Chem. Lett. 2010, 1, 3027–3032

by the crowders is much smaller than that caused by an equivalent increase in peptide concentration (Figure 5, right). Moreover, this discrepancy grows by increasing the aggregation propensity (i.e., at higher dE) and is similar to the one previously observed in the trend of the t_{N^*} for different values of dE (see Figure 3). The different effects of crowders and peptide concentration have not been observed previously. It would be interesting to validate them by kinetic measurements on peptides that aggregate very fast like diphenylalanine.[26]

Two Main Scenarios of Aggregation. The aggregation kinetics of a simple model of an amphipathic peptide have been investigated at different concentrations of inert crowders. The excluded volume effect stabilizes larger oligomers (Figures 2 and 4). However, at high crowder content, the solution becomes more viscous (Figure S1, Supporting Information), and the peptide mobility decreases because each monomer is locally confined by the crowders (see Table 1). The confinement decreases the rate of monomer encounters and, therefore, association (Figures 3 and 5). Two main scenarios emerge from the present simulation study.

For peptides with low aggregation propensity, the self-association process is transition-state-limited, where the kinetic bottleneck is the formation of the fibril nucleus. In this case, since the oligomers, including the nucleus, are thermodynamically favored (with respect to the isolated monomers) by the excluded volume effect, macromolecular crowding accelerates peptide assembly and has an effect analogous to that of an increase in peptide concentration (Figure 5, left).

On the other hand, when the aggregation mechanism is fast and proceeds directly from monomers to the fibril, the process is diffusion-limited, and the thermodynamic stabilization of oligomers is less important than the reduction in peptide mobility. In this case, the bottleneck is not the formation of the nucleus; the rate-limiting step for peptides that show a direct aggregation mechanism is the elongation of the fibril. Therefore, in this case, macromolecular crowding is much less efficient in accelerating peptide self-association than an equivalent increase of the peptide concentration since the peptides motion is hindered by the crowders (Figure 5, right). The very different relative influence of crowders and concentration observed in the simulations is a new finding which suggests that kinetic experiments at different crowder contents might discriminate between different mechanisms of aggregation, that is, downhill from barrier-limited.

METHODS

Peptide Model. The amphipathic peptide model adopted here has been described in detail elsewhere.[22] Briefly, each peptide monomer consists of 10 beads. Four of the beads carry partial charges of $\pm 0.4e$, thereby generating two dipoles. Four of the uncharged spheres are hydrophilic, and the other two are hydrophobic. Interactions between monomers depend on van der Waals and electrostatic forces. The former approximate both steric and hydrophobic effects, while the latter are specific dipole−dipole interactions responsible for the ordered stacking of monomers incorporated in the fibril. A parallel polar contact is formed whenever two charged beads of different monomers are closer than 5 Å. Different aggregation pathways are obtained by changing the relative stability of the amyloid-competent (β) and amyloid-protected (π) states, which are ruled by the dihedral energy difference of the single rotatable bond of the monomer. The energy difference of these two states, $dE = E_\pi - E_\beta$, can be therefore interpreted as the β-aggregation propensity of the polypeptide. Since the peptide has only one degree of freedom, dE is close to the free-energy difference between the two aforementioned states. For instance, when $dE = 0$ kcal/mol, the π and β states are equally populated, whereas for $dE = -1.5$ and -2.5 kcal/mol, the π state is about 15 and 100 times more populated than the β state, respectively.

Crowder Model. The crowders are neutral spherical particles that interact with the peptides and with each other by means of the Lennard-Jones potential, given by the following equation

$$V_{ij} = \epsilon_{ij}^{\min}\left[\left(\frac{R_{ij}^{\min}}{r_{ij}}\right)^{12} - 2\left(\frac{R_{ij}^{\min}}{r_{ij}}\right)^{6}\right] \qquad (1)$$

where $R_{ij}^{\min}$ is the distance at the minimum of the potential, or the van der Waals radius of the molecule, $\epsilon_{ij}^{\min}$ is the depth of the potential well, and r_{ij} is the interparticle distance. The value of $R_{ij}^{\min}$ is set to 7.5 Å, and $\epsilon = 0.1$ kcal/mol for the crowders, which therefore behave as impenetrable soft spheres. The mass of the crowders has been set to 6.5 kDa. The interactions between the crowder and peptide are also modeled with a Lennard-Jones potential. In this case, the $\epsilon_{ij}^{\min}$ parameter is set to 0.01 kcal/mol to make the crowders softly repulsive particles; the optimal distance is obtained by using the arithmetic mean.

Simulation Protocol with Crowders. Each simulated system is made up of 125 peptides in a cubic box of size equal to 290 Å, at a peptide concentration of 8.5 mM and a variable number of crowders (see Table 1). Periodic boundary conditions are imposed. All of the simulations were carried out at 310 K by means of Langevin dynamics using CHARMM.[27,28] Since aggregation is a stochastic process, 10 simulations with different starting velocities were run for every concentration of crowders and for each value of the β-aggregation propensity of the peptides. The time interval for saving the coordinates of the system was 0.5 ns. It is important to note that the relative populations of β and π states of the isolated monomer are influenced solely by the value of dE and not by the crowder content because the interactions between crowders and peptides are not sensitive to the two different states of the monomers.

Simulation Protocol without Crowders. These simulations were carried out as described above (i.e., 125 peptides and 310 K) in the absence of crowders and using box sizes ranging from 150 to 290 Å, corresponding to a peptide concentration ranging from 61.5 to 8.5 mM, respectively.

Excluded Volume. A rigorous protocol to calculate the volume fraction that the crowders exclude to peptides at different concentrations has been established. According to

DOI: 10.1021/jz100967z | J. Phys. Chem. Lett. 2010, 1, 3027–3032

the linear approximation, the excluded volume fraction is given by the following equation

$$\phi^{I}(n_C) = \frac{V_{excl}}{V_{tot}} = \frac{1}{V_{tot}}\frac{4}{3}\pi R_{eff}^3 n_C$$

where $R_{eff} = R_C + R_P$ is the sum of the radius of the crowder R_C and the radius of the peptide R_P and n_C is the number of crowders in the total volume. This approximation holds only if the crowders are significantly larger than the peptide, that is, when $R_{eff} \approx R_C$. If the radius of the peptides is non-negligible, the excluded volume must include two corrections arising from the presence of crowders whose mutual distance is lower than $2R_{eff}$ (see Figure S2, Supporting Information).

Since the peptide is not fully spherical, a heuristic evaluation of R_{eff} is needed. A simulation of an "ideal" solution mixture of 125 peptides and 500 crowders was run, where the polar interactions of the peptides were switched off, as well as the hydrophobic ones, to prevent them from aggregating. From a 500 ns run, the radial distribution functions $g(r)$ for each pair of species in the solution were calculated. The effective radius R_{eff} has been chosen as the radius where the radial distribution function $g_{CP}(r)$ between the crowders and the peptides has the value of 0.5 (cfr. Figure S3, Supporitng Information), obtaining $R_{eff} = 11.6$ Å. The effective excluded volume fraction ϕ is calculated by dividing the whole simulation box in "infinitesimal" cubic elements and counting the number of cubes whose distance from any crowder particles center is less than R_{eff}, which is the minimal approachable distance between a crowder and a peptide.

Simulations of 500 ns with different numbers of crowders were used to produce snapshots of the system with different arrangements of the crowders. The excluded volume fraction ϕ at different crowder content n_C, reported in Table 1, is calculated as an average over all snapshots of the simulations. The equivalent concentration $C_{eq} = 8.5\ \text{mM}/(1 - \phi)$ is the concentration of peptides in the accessible volume.

Dimension of the Fibril Nucleus. The nucleus is defined as the oligomer that has 50% probability to form a fibril.[22] The crucial feature of such an oligomer is that it is not only formed by a certain number of monomers but that it also owns the sufficient number of monomers in the β state to permit the elongation of the fibril (Table S1, Supporting Information).

Self-Diffusion Coefficient. The self-diffusion coefficient $\mathcal{D}$, which measures the mobility of the isolated peptides, can be calculated through the Einstein relation

$$\lim_{t \to \infty} \langle r^2(t) \rangle = 6\mathcal{D}t$$

where $\langle r^2(t) \rangle$ is the mean-square displacement. Simulations of 100 ns with different concentrations of crowders and 125 peptides were performed to calculate the mean-square displacement functions. The polar and the hydrophobic interactions of the peptides were switched off to prevent aggregation events and calculate the diffusivity of the single monomers. The self-diffusion coefficients of peptides at different crowder contents $\mathcal{D}(n_C)$ (Table 1) were then derived by a linear fit of the long-time behavior of the mean-square displacement (see Figure S4, Supporting Information).

SUPPORTING INFORMATION AVAILABLE

Supplementary Figures 1−4 and Table 1. This material is available free of charge via the Internet at http://pubs.acs.org.

AUTHOR INFORMATION

Corresponding Author:

*To whom correspondence should be addressed. E-mail: caflisch@bioc.uzh.ch (A.C.); pellarin@bioc.uzh.ch (R.P.).

ACKNOWLEDGMENT This work was supported by a grant of the Swiss National Science Foundation to A.C. The simulations were carried out on the Schrödinger compute cluster of the University of Zürich.

REFERENCES

(1) Dobson, C. M. Protein Folding and Misfolding. *Nature* **2003,** *426*, 884–890.
(2) Lansbury, P. T.; Lashuel, H. A. A Century-Old Debate on Protein Aggregation and Neurodegeneration Enters the Clinic. *Nature* **2006,** *443*, 774–779.
(3) Fowler, D. M.; Koulov, A. V.; Balch, W. E.; Kelly, J. W. Functional Amyloid — From Bacteria to Humans. *Trends Biochem. Sci.* **2007,** *32*, 217–224.
(4) Maji, S. K.; Perrin, M. H.; Sawaya, M. R.; Jessberger, S.; Vadodaria, K.; Rissman, R. A.; Singru, P. S.; Nilsson, K. P. R.; Simon, R.; Schubert, D.; et al. Functional Amyloids As Natural Storage of Peptide Hormones in Pituitary Secretory Granules. *Science* **2009,** *325*, 328–332.
(5) Kraineva, J.; Smirnovas, V.; Winter, R. Effects of Lipid Confinement on Insulin Stability and Amyloid Formation. *Langmuir* **2007,** *23*, 7118–7126.
(6) Mittal, J.; Best, R. B. Thermodynamics and Kinetics of Protein Folding under Confinement. *Proc. Natl. Acad. Sci. U.S.A.* **2008,** *105*, 20233–20238.
(7) Fulton, A. B. How Crowded Is the Cytoplasm. *Cell* **1982,** *30*, 345–347.
(8) Zimmerman, S. B.; Trach, S. O. Estimation of Macromolecule Concentrations and Excluded Volume Effects for the Cytoplasm of Escherichia-Coli. *J. Mol. Biol.* **1991,** *222*, 599–620.
(9) Ellis, J. R. Macromolecular Crowding: Obvious but Underappreciated. *Trends Biochem. Sci.* **2001,** *26*, 597–604.
(10) Minton, A. P. The Influence of Macromolecular Crowding and Macromolecular Confinement on Biochemical Reactions in Physiological Media. *J. Biol. Chem.* **2001,** *276*, 10577–10580.
(11) Zhou, H. -X.; Rivas, G.; Minton, A. P. Macromolecular Crowding and Confinement: Biochemical, Biophysical, And Potential Physiological Consequences. *Ann. Rev. Biophys.* **2008,** *37*, 375–397.
(12) Lebowitz, J. L.; Rowlinson, J. S. Thermodynamic Properties of Mixtures of Hard Spheres. *J. Chem. Phys.* **1964,** *41*, 133–138.
(13) Minton, A. P. Models for Excluded Volume Interaction between an Unfolded Protein and Rigid Macromolecular Cosolutes: Macromolecular Crowding and Protein Stability Revisited. *Biophys. J.* **2005,** *88*, 971–985.
(14) Ellis, R. J.; Minton, A. P. Protein Aggregation in Crowded Environments. *Biol. Chem.* **2006,** *387*, 485–497.
(15) Cheung, M. S.; Klimov, D.; Thirumalai, D. Molecular Crowding Enhances Native State Stability and Refolding Rates of Globular Proteins. *Proc. Natl. Acad. Sci. U.S.A.* **2005,** *102*, 4753–4758.

DOI: 10.1021/jz100967z | *J. Phys. Chem. Lett.* **2010,** *1*, 3027–3032

(16) Mittal, J.; Best, R. B. Dependence of Protein Folding Stability and Dynamics on the Density and Composition of Macromolecular Crowders. *Biophys. J.* **2010,** *98*, 315–320.
(17) Auer, S.; Trovato, A.; Vendruscolo, M. A Condensation-Ordering Mechanism in Nanoparticle-Catalyzed Peptide Aggregation. *PLoS Comput. Biol.* **2009,** *5*, 1–7.
(18) Munishkina, L. A.; Cooper, E. M.; Uversky, V. N.; Fink, A. L. The Effect of Macromolecular Crowding on Protein Aggregation and Amyloid Fibril Formation. *J. Mol. Recognit.* **2004,** *17*, 456–464.
(19) Munishkina, L. A.; Ahmad, A.; Fink, A. L.; Uversky, V. N. Guiding Protein Aggregation with Macromolecular Crowding. *Biochemistry* **2008,** *47*, 8993–9006.
(20) Zhou, B. -R.; Zhou, Z.; Hu, Q. -L.; Chen, J.; Liang, Y. Mixed Macromolecular Crowding Inhibits Amyloid Formation of Hen Egg White Lysozyme. *Biochim. Biophys. Acta* **2008,** *1784*, 472–480.
(21) Zhou, Z.; Fan, J. -B.; Zhu, H. -L.; Shewmaker, F.; Yan, X.; Chen, X.; Chen, J.; Xiao, G. -F.; Guo, L.; Liang, Y. Crowded Cell-Like Environment Accelerates the Nucleation Step of Amyloidogenic Protein Misfolding. *J. Biol. Chem.* **2009,** *284*, 30148–30158.
(22) Pellarin, R.; Caflisch, A. Interpreting the Aggregation Kinetics of Amyloid Peptides. *J. Mol. Biol.* **2006,** *360*, 882–892.
(23) Pellarin, R.; Guarnera, E.; Caflisch, A. Pathways and Intermediates of Amyloid Fibril Formation. *J. Mol. Biol.* **2007,** *374*, 917–924.
(24) Friedman, R.; Pellarin, R.; Caflisch, A. Amyloid Aggregation on Lipid Bilayers and Its Impact on Membrane Permeability. *J. Mol. Biol.* **2009,** *387*, 407–415.
(25) Friedman, R.; Pellarin, R.; Caflisch, A. Soluble Protofibrils As Metastable Intermediates in Simulations of Amyloid Fibril Degradation Induced by Lipid Vesicles. *J. Phys. Chem. Lett.* **2010,** *1*, 471–474.
(26) Reches, M.; Gazit, E. Designed Aromatic Homo-Dipeptides: Formation of Ordered Nanostructures and Potential Nanotechnological Applications. *Phys. Biol.* **2006,** *3*, S10–S19.
(27) Brooks, B. R.; Bruccoleri, R. E.; Olafson, B. D.; States, D. J.; Swaminathan, S.; Karplus, M. CHARMM — A Program for Macromolecular Energy, Minimization, And Dynamics Calculations. *J. Comput. Chem.* **1983,** *4*, 187–217.
(28) Brooks, B. R.; Brooks, C. L.; Mackerell, A. D.; Nilsson, L.; Petrella, R. J.; Roux, B.; Won, Y.; Archontis, G.; Bartels, C.; Boresch, S.; et al. CHARMM: The Biomolecular Simulation Program. *J. Comput. Chem.* **2009,** *30*, 1545–1614.

DOI: 10.1021/jz100967z | *J. Phys. Chem. Lett.* **2010,** *1*, 3027–3032